Effects of Strake Position on the Flow past an Inclined Ogive Cylinder

Y. T. Ng,* S. C. Luo,† and T. T. Lim†
National University of Singapore, Singapore 119260, Republic of Singapore

I. Introduction

THERE is much interest surrounding the study of the flowfield past an inclined ogive cylinder. Through the exhaustive works of Lamont,[1] Zilliac,[2] Degani and Zilliac,[3] and Luo et al.,[4] it is well known that such flows are dominated by the formation of a pair of trailing vortices. Depending on the angle of attack of the ogive model, symmetric trailing vortices (for low angles of attack) or asymmetric trailing vortices (for high angle of attack) can be generated. It is well established that the asymmetric vortices induce a large side force on the ogive cylinder, and the side force switches direction at distinct roll angles, thereby giving rise to the well-known square-wavelike distribution. To compound this problem further, such flows are highly sensitive to microsurface imperfections.[5] Hence, one is unable to predict accurately the roll angles at which the side force crosses over, even for similar looking ogive cylinders.

Different flow control techniques have been proposed to address these problems. These include the use of boundary-layer trips, surface roughening techniques, the rounding of the ogive nose tip, and the use of finlike structures or strakes. Stahl[6] and Asghar et al.[7] demonstrated that the use of a single vertical strake placed at the tip and at the leeside of a conical cylinder can reduce the side force exerted on their cylinder model. Essentially, the strake isolates the interaction between the two vortices at the tip and thereby promotes the formation of a pair of symmetric trailing vortices. Ng[8] used dye flow visualization techniques to show that the presence of a strake, at an ogive tip, resulted in the formation of symmetric trailing vortices.

Although research work on the use of a strake as a flow control technique is well documented, the effects of strake position on the side force are less readily available. In this experiment, a single triangular strake was placed at different positions from the tip to ascertain its effects on the measured side force. Surface oil flow visualization was also used to study qualitatively the separation position near the tip. Similar techniques were used by Degani et al.[9] to study the surface flow pattern of a strake-free ogive cylinder.

II. Experimental Setup

The experimental apparatus and procedures have been described in detail in Ref. 4 and will only be briefly introduced here. The experiment was performed in an open-loop wind tunnel with a rectangular test section measuring 0.6 m (height) × 1.0 m (width), operating at a freestream velocity U of 15 m/s. The Reynolds number Re based on the model diameter ($D = 0.035$ m) was about 3.5×10^4. At this Reynolds number, the boundary layer involved is likely to be laminar, and laminar separation is expected to occur on the model at all of the angles of incidences investigated. Two angles of attack α were considered, that is, 45 and 50 deg, and were chosen based on the knowledge that the side-force coefficient C_{Fy} vs roll angle ϕ distribution exhibits a square-wavelike pattern in this α range. A force balance was used to measure the overall side force, and a computer-controlled stepper motor was used to initiate a rolling motion for the model at discrete angular increments of 7.2 deg.

A single triangular strake was used in the present study, and its dimensions are given in Fig. 1. Also, in Fig. 1 are the dimensions of the ogive tip and the definition of the coordinate system used. The tip-to-strake distance in the x_s direction, that is, x_s/D, where x_s is the axis along the axial direction of the model, is measured with a vernier calliper from the apex of the ogive tip to the leading apex of the triangular strake. The leading edge of the strake is sharpened and placed vertically at the leeward side of the ogive tip at different x_s/D locations. The side force is then measured for each strake location.

To check the effectiveness of the strake in controlling vortex asymmetry, the side force acting on a strake-free ogive tip was also measured. The reference side-force coefficient for each angle of attack is designated C_{Fy0}, whereas the corresponding coefficient with the strake is designated C_{Fys}.

Oil surface flow visualization was performed to study the flow separation location corresponding to different strake position. Carbon chalk, which had been ground and sieved, was mixed with commercially available acrylic flow enhancer (Cryla Flow Enhancer by Daler Rowney), and the mixture was applied thinly to the model with a small paintbrush. The running time was about 10 min, after which the ogive tip was removed and photographs were taken.

III. Results and Discussion

For the strake-free ogive model, Fig. 2 shows the variation of C_{Fy} with ϕ at $\alpha = 45$ and 50 deg. The typical square-wave responses for both cases are clearly seen and are similar to those obtained by Degani and Zilliac[3] and Luo et al.[4] The C_{Fy} data from Luo et al.[4] are also plotted in Fig. 2 for comparison. The reference side force coefficients C_{Fy0} at $\phi = 0$ deg for $\alpha = 45$ and 50 deg are 3.77 and 3.99, respectively.

In all cases, force measurements were conducted at one fixed roll angle, namely, $\phi = 0$ deg. To illustrate the effects of the strake position on the side force, all measured C_{Fys} data at different α are normalized with their respective C_{Fy0}. Figure 3 shows the variations of the normalized side force (C_{Fys}/C_{Fy0}) for different strake locations ranging from $x_s/D = 0.0$ to $x_s/D = 0.71$. Note that at $x_s/D = 0.0$ for both $\alpha = 45$ and 50 deg, the resulting side force C_{Fys} is reduced significantly and can be attributed to the formation of less asymmetric trailing vortices[8] because the placement of the

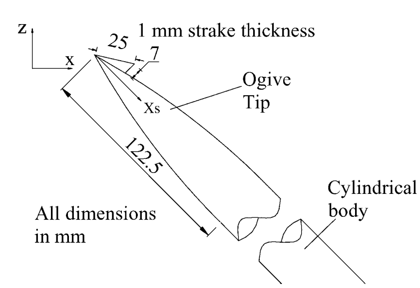

Fig. 1 General dimensions of the ogive tip and triangular strake.

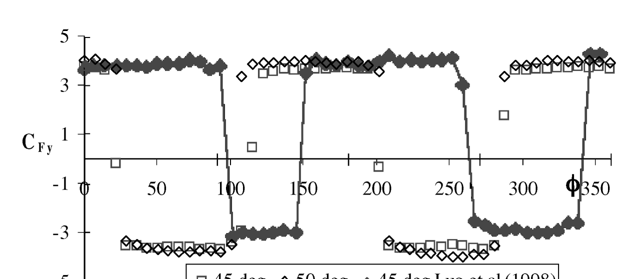

Fig. 2 Square-wavelike variation of C_{Fy} with ϕ at α = 45 and 50 deg.

Received 21 February 2003; revision received 27 August 2003; accepted for publication 24 September 2003.

*Research Engineer, Department of Mechanical Engineering.
†Associate Professor, Department of Mechanical Engineering.

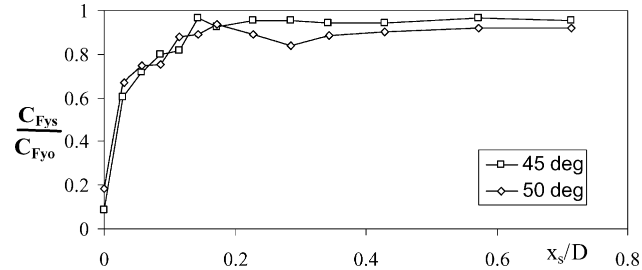

Fig. 3 Variation of C_{Fys}/C_{Fy0} with tip-to-strake distance (x_s/D); C_{Fy0} and C_{Fys} refer to the side force coefficient at $\phi = 0$ only, for $\alpha = 45$ and 50 deg, C_{Fy0} are 3.77 and 3.99, respectively.

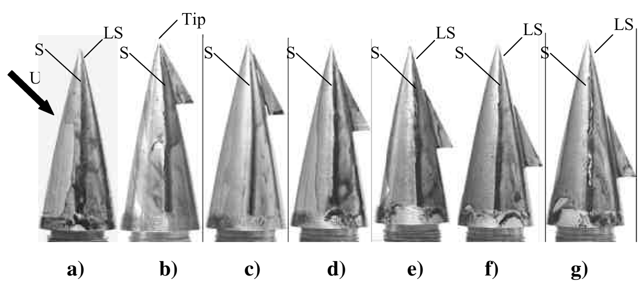

Fig. 4 Oil surface flow visualization of ogive tip at $\alpha = 45$ deg for different strake positions (arrow indicates the general flow direction): a) no strake, b) $x_s/D = 0.0$, c) $x_s/D = 0.11$, d) $x_s/D = 0.23$, e) $x_s/D = 0.34$, f) $x_s/D = 0.57$, and g) $x_s/D = 0.71$.

strake isolates the interaction of the rolled-up vortices near the tip. As x_s/D increases, the side force increases asymptotically to that found in the strake-free ogive model. This suggests that at larger x_s/D, the strake is gradually being enveloped by the wake of the ogive cylinder and has lost its effectiveness in attenuating the magnitude of the side force. The initial vortex asymmetry that develops near the nose tip is propagated downstream and forms a pair of asymmetric trailing vortices.

To shed more light on the influence of a strake on the flow over the ogive cylinder, we carried out an oil surface flow visualization for similar tip-to-strake distances at $\alpha = 45$ deg, and the results are shown in Figs. 4a–4g. Because the model was inclined during the test, an arrow is included in Fig. 4 to indicate the general flow direction. All separation lines are labeled with a letter S. An overall inspection of Fig. 4 shows that the separation lines are almost straight, except for some separation lines that are noted to have a slight curvature, for example, Figs. 4b and 4c. On closer inspection of the flow visualization, the strake-free ogive tip in Fig. 4a shows that the separation line is straight and that at the position that is labeled *LS* (for leeside), the separation line connects continuously to its counterpart on the opposite side of the model. To provide a clearer explanation, a schematic is presented in Fig. 5 to show the different cross-sectional vortical structures and the location of the separation line near the nose tip. A similar schematic was also presented by Rom.[10] In the immediate vicinity of the nose tip in section A–A, where the cylinder's diameter is small, a symmetric cross-sectional flow pattern arises without flow separation and, hence, an absence of separation lines is expected. At a greater distance from the nose tip at sections B–B and C–C, a symmetric flow pattern with separation develops initially (in section B–B), and the vortical structure later evolves into an asymmetrical one (in section C–C). The presence of flow separation in these two locations indicates that the presence of separation lines and the evidence presented in the corresponding flow visualization of Fig. 4a support the qualitative description given in the schematic.

On addition of the strake at $x_s/D = 0.0$ and 0.11, as shown in Figs. 4b and 4c, respectively, the separation lines appear to be

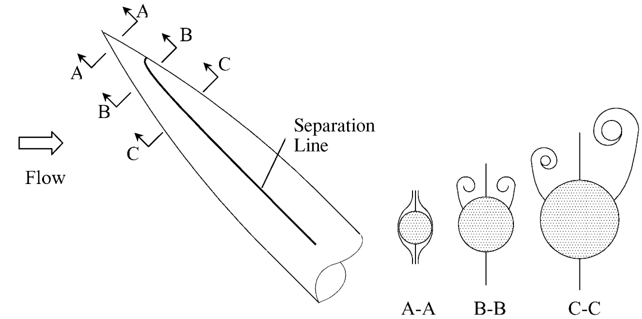

Fig. 5 Schematic showing cross-sectional vortical structure near the tip and its relation to the separation line.

curved, and the presence of the strake resulted in the isolation of the separation line on both sides of the model. The separation line on the two sides of the model do not seem to be connected to each other. With further increases in x_s/D to 0.23, 0.34, 0.57, and 0.71, the effects of the strake diminishes, and the separation line straightens. The separation line on both sides of the model reconnects near the tip at position *LS* in Figs. 4e–4g.

IV. Conclusions

The effectiveness of the use of different strake positions to control vortex asymmetry is investigated. The results show that a strake placed at the tip of the nose can cause a significant reduction in the side force acting on the ogive cylinder. However, its effectiveness decreases with downstream distance, and the side force asymptotes to that of the strake-free ogive cylinder. Oil surface flow visualization reveals that the presence of a strake alters the position and the shape of the separation line. Without the strake, the separation line originates slightly downstream of the tip, whereas with the strake placed at the tip, it appears to start at the tip. This finding suggests that the strake at the tip not only minimizes the interaction of the tip vortices, but also forces the origin of the separation line to move to the tip, which had not been reported previously.

References

[1] Lamont, P. J., "Pressures Around an Inclined Ogive Cylinder with Laminar, Transitional, or Turbulent Separation," *AIAA Journal*, Vol. 20, No. 11, 1982, pp. 1492–1499.

[2] Zilliac, G. G., "Computational/Experimental Study of the Flowfield on a Body of Revolution at Incidence," *AIAA Journal*, Vol. 27, No. 8, 1989, pp. 1008–1016.

[3] Degani, D., and Zilliac, G. G., "Experimental Study of Nonsteady Asymmetric Flow Around an Ogive Cylinder at Incidence," *AIAA Journal*, Vol. 28, No. 4, 1990, pp. 642–649.

[4] Luo, S. C., Lim, T. T., Lua, K. B., Chia, H. T., Goh, E. K. R., and Ho, Q. W., "Flowfield Around Ogive/Elliptic-Tip Cylinder at High Angle of Attack," *AIAA Journal*, Vol. 36, No. 10, 1998, pp. 1778–1787.

[5] Degani, D., "Effects of Geometrical Disturbance on Vortex Asymmetry," *AIAA Journal*, Vol. 29, No. 4, 1991, pp. 560–566.

[6] Stahl, W., "Suppression of Vortex Asymmetry Behind Circular Cones," *AIAA Journal*, Vol. 28, No. 6, 1990, pp. 1138–1140.

[7] Asghar, A., Stahl, W. H., and Mahmood, M., "Suppression of Vortex Asymmetry and Side Force on a Circular Cone," *AIAA Journal*, Vol. 32, No. 10, 1994, pp. 2117–2120.

[8] Ng, T. T., "Effects of a Single Strake on the Forebody Vortex Asymmetry," *Journal of Aircraft*, Vol. 27, No. 9, 1990, pp. 844–846.

[9] Degani, D., Tobak, M., and Zilliac, G. G., "Surface Flow Patterns on an Ogive–Cylinder at Incidence," *AIAA Journal*, Vol. 30, No. 1, 1992, pp. 272–274.

[10] Rom, J., *High Angle of Attack Aerodynamics. Subsonic, Transonic and Supersonic Flows*, Springer-Verlag, New York, 1992, pp. 23–29.

W. Devenport
Associate Editor